Semnan University

Progress in Engineering Thermodynamics and Kinetics Journal

Journal homepage: https://jpetk.semnan.ac.ir/

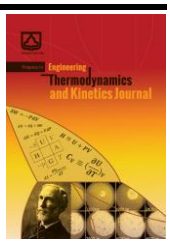

Research Article

An Overview of Determination of Young's modulus by AFM in Various Fields

Maryam Daraee [a *], Sedigheh Sadegh Hassani [b,c], Somayeh Jalilzadeh Azar [c,d]

[a] *Nano Compound Seman Dara Company, Mahdishahr, Semnan, Iran*
[b] *Catalysis Research Division, Research Institute of Petroleum Industry (RIPI), Tehran, Iran*
[c] *Iran Laboratory Network, SPM Experts work group*
[d] *M.Sc. Microbiology, Chemistry & Chemical Engineering Research Center of Iran, Tehran, Iran*

ARTICLE INFO

Article history:

Received: 202*-**-**
Revised: 202*-**-**
Accepted: 202*-**-**

Keywords:

Atomic force microscope;
Young's modulus;
Force curve;
Elasticity;
Stress;
Strain.

ABSTRACT

The Atomic Force Microscope (AFM) is a powerful tool for studying the properties and structures of materials at the nanometer scale. Unlike most surface analysis methods, it has no restrictions on the type of surface or its environment. This versatility enables AFM to investigate a wide range of materials, including conductive, insulating, soft, hard, cohesive, powdered, biological, organic, and inorganic substances. As such, it finds applications in diverse scientific fields, including chemistry, surface chemistry, polymer science, physics, molecular engineering, semiconductor science, biology, and medicine. Beyond its ability to image surfaces, AFM can also measure mechanical properties like Young's modulus. Young's modulus, also known as the modulus of elasticity (E), is defined as the ratio of stress to strain in the elastic region. This value reflects the stiffness of a material and changes with temperature. This paper examines the application of atomic force microscopy (AFM) in measuring Young's modulus across various scientific disciplines.

*** Corresponding author.**
E-mail address: m20.daraee@gmail.com

Cite this article as:

Daraee. M., Sadegh Hassani, S., & Jalilzadeh Azar, S. (2025). An Overview of Determination of Young's modulus by AFM in Various Fields. *Progress in Engineering Thermodynamics and Kinetics*.

https://doi.org/10.22075/jpetk.2024.27737.1011

1. Introduction

Young's modulus as one of the most important mechanical properties of materials is defined as the elastic properties of a solid substance that it undergoing tension or compression in only one direction, which sometimes it nominated as elasticity, it is named after the Thomas Young (one of the 19th century British scientists) [1-2].

The modulus of elasticity is actually the ratio of stress to strain of a substance, and it is a constant value for each material. Modulus of elasticity is used as a way to identify different materials. Recently, atomic force microscopy (AFM) has been used as a quantitative characterization technique to determine surface mechanical properties. The atomic force microscope is a powerful non-destructive tool for imaging the surface topography with nanometric resolution. Additionally, by AFM, information about friction behavior, thermal properties, and surface elasticity can be obtained that cannot be achieved using other methods. This microscope typically does not require the very high vacuum commonly used in TEM and SEM [3-5]. It can be used to determine the Young's modulus of substrates by studying the interaction between the tip and surface [6-9]. Moreover, the mechanical properties of cells or tissues in biological and non-biological systems can be investigated using AFM.

2. Young's modulus

Young's modulus, as a fundamental material property, describes the elastic properties of a solid under tension or compression in one direction, which shows a solid's stiffness or resistance to elastic deformation under load. The influence of strains on the under-load material leads to the displacement of the structure.

Young's modulus is the ratio of tensile stress to tensile strain along a line, where stress and strain are defined as force per unit area and proportional deformation, respectively. Figures 1a and 1 b show the effect of stiffness on the Young's modulus value with a change in length, respectively. A uniaxial stress (extension or compression) is given to a material with low stiffness (green Fig.1-a) and high stiffness (blue Fig. 1-a), which can cause their deformation [10-11].

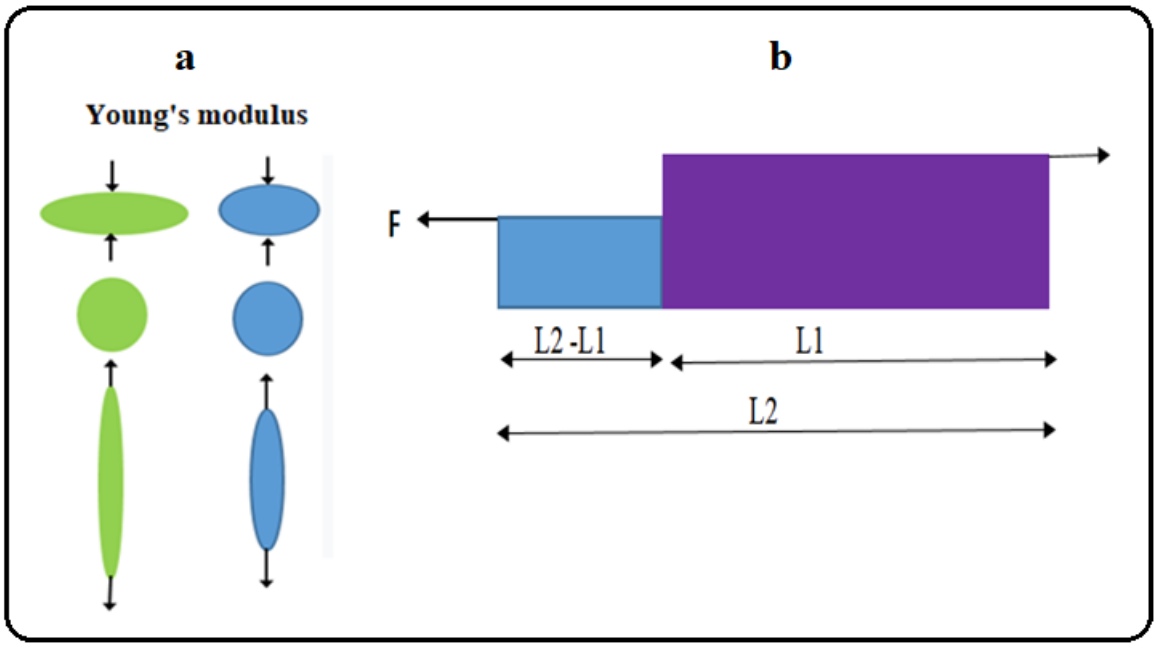

Figure 1: Effect of stiffness on Young's modulus value.

By compressing or extending materials, elastic deformation occurs, which will return to its original shape when the load is removed. Flexible materials or elastic solids show a low Young's modulus value, and stiff materials or inelastic solids indicate a high Young's modulus.

The equation for Young's modulus is:

$$E = \text{stress/strain} = \sigma / \varepsilon = (F/A) / (\Delta L/L_1) = FL_1 / A\Delta L$$

Where E, σ, and ε are Young's modulus (Pa), the uniaxial stress and the strain, F defined as the force of compression or extension, A is the cross-sectional surface area perpendicular to the applied force, Δ L and L are the change in length (negative under compression; positive when stretched) and the original length, respectively. L_2 is the new length (Fig. 1-b).

2.1. Atomic Force Microscope

The Atomic Force Microscope can be used to measure several properties, including surface morphology, adhesion and friction forces, elasticity, magnetic properties, distribution of electric charges, and electrical polarity of different points. These capabilities are used to evaluate properties such as roughness, uniformity, adhesion, corrosion, friction, size, and others, which are applied in various fields and industries, including chemistry, physics, materials and metallurgy, polymer engineering, biology, and medicine [12-16].

The AFM works by bringing the cantilever tip close to the sample surface. A laser beam reflects off the backside of the cantilever, and a photodiode records its position. Any attractive or repulsive forces between the tip and the surface cause the cantilever to bend, changing the direction of the reflected beam. The detector measures the amount of this deflection, allowing us to generate a topographic map of the sample surface with nanometer-scale resolution in the X and Y directions and angstrom-level resolution in the Z direction [17-19].

Using the AFM, it is possible to make nanometer-scale changes in sample surfaces using both mechanical and chemical methods. Among the AFM capabilities, making nano-indentation is also essential, which is a valuable capability for Young's modulus investigation. AFM would be able to monitor the surface via in situ imaging of the indentation without switching equipment [20]. Several factors influence the calculation of Young's modulus using AFM, including temperature changes, cantilever shape and geometry, and beam shape. This technique can be applied to a wide range of materials, including rubber, polymers, metals, glasses, alloys, carbon nanotubes, graphene, and diamond. Generally, solids possess high Young's moduli, while elastomers have low values.

The calculation involves determining the slope of the linear portion of the stress-strain curve. For simplicity, the Hertz model is a recommended approach for extracting the necessary quantities. This requires obtaining the dimensions of the cantilever tip (length, width, thickness, and radius) using calibration samples and scanning electron microscope (SEM) images [20].

The cantilever's response is recorded after introducing the modulation signal to the sample using the responsive phase and amplitude. Young's modulus can be calculated by phase and amplitude versus driving frequency. Additionally, it can be obtained from the resonance frequencies between the tip-surface interaction and the Young's modulus, or the modulus of elasticity, which is calculated by determining the force created at the resonance frequency of the sample [21].

3. Hertz model

In 1881, Heinrich Hertz presented the Hertz model, in which the tip and the sample are assumed to be two spheres by considering elastic deformation with radius R1 and radius R2, respectively. So, both the interpenetration between surfaces during the indentation process and any F_a acting between the surface and the AFM tip are ignored [20].

Applying this model is only possible if the probe indentation value into the sample surface is significantly smaller than the tip curvature radius, thereby eliminating plastic deformations in the sample surface. Finding the contact point between the tip and the sample surface is so vital in force F measurement, dependent on the indentation value δ [22].

However, the equation in this model is summarized in the following formula:

$$A_c = \pi \left(\frac{RF}{K}\right)^{2/3}$$

R is obtained by incorporating the curvature radius of different materials, and K is related to their combined elastic modulus, which is formulated as follows:

$$K = \frac{4}{3}\left(\frac{1-v_i^2}{E_i} + \frac{1-v^2}{E}\right)^{-1}$$

E is the Young's modulus, and ν is the Poisson ratio for the material and the indenter.

Johnson, Kendall, and Roberts [23] designed a mechanics model for calculating A_c, as follows:

$$\gamma = \gamma_1 + \gamma_2 - \gamma_{12}$$

ϒ is the work per unit of area that is necessary to separate the tip and surface. Υ_1 and Υ_2 are the surface energies of the sample and surface, Υ_{12} is the interfacial energy. This model is more credible for sticky surfaces and tips with a large R, and interaction forces are ignored. According to this model, A_c is formulated as:

$$A_c = \pi \frac{R^{2/3}}{K^{2/3}}\left(F + 3\pi\gamma R + \sqrt{6\pi\gamma RF + (3\pi\gamma R)^2}\right)^{2/3}$$

When the value of ϒ tends to zero, the above equation approaches the Hertz model.

4. Application of AFM in the determination of Young's modulus

Atomic force microscopy is a strong tool for studying a wide range of materials at the nanoscale. Using this microscope, it is possible to study the structural, physical, and mechanical properties of materials such as roughness, hardness, Young's modulus, topography, and particle size, as well as force determination on a nano-Newton scale.

It can be applied in various fields, such as chemistry, materials science, physics, polymer science, Semiconductor Technology, and other sciences. Imaging of biomolecules in physiological conditions is one of the capabilities of AFM, which makes this technique widely used in biology and medicine, too.
This device can also perform nanoindentation investigations and change the particles and sample surfaces [24-28]. This article briefly describes some of the most important uses of the AFM in Young's modulus determination in various fields.

5. Application of AFM in the Young's modulus determination in the biological science

Understanding the mechanical properties of biological tissues is crucial for detecting disease states, maintaining tissue homeostasis, and guiding reconstructions. Mesenchymal stromal/stem cells (MSCs) derived from human tissues have demonstrated therapeutic potential in various applications, including bone and tissue formation, repair, reconstruction, and cell therapy. Notably, MSCs are known to be sensitive to mechanical cues such as shear stress and matrix stiffness. Atomic force microscopy (AFM) presents a powerful tool to measure the cellular stiffness of live human MSCs through appropriate biological sample preparation.

Using AFM, we can obtain three-dimensional images of these samples at the nanometer scale and calculate the Young's modulus, a parameter reflecting the cell's stiffness. By employing a conical silicon tip cantilever with a spring constant of k = 0.03 N/m, we can measure the average Young's modulus of the MSCs [29]. Some researches were done on nanomaterials. Mazzini et al .exhibited nano-mechanical properties and average Young's modulus of internal limiting membrane under Ocriplasmin treatment by the AFM. They determined the nano-mechanical properties of a kind of membrane by treating a type of syndrome with a drug called Ocriplasmin. They understood a time-dependent increase of the Young's modulus over time of about 19% of its value in 30 min, up to reach a maximum value [30]. This research produced bio-nanocomposite films for wound dressing applications using gellan gum (GG) and titanium dioxide nanotubes (TiO_2-NTs) via the evaporative casting method. The authors investigated the mechanical properties, antibacterial activity, and chemical interactions between TiO2 nanotubes (NTs) and GG. Their results indicate that incorporating TiO2-NTs improves the mechanical properties of the GG films due to their uniform dispersion within the matrix. While increasing the concentration of TiO_2-NTs reduces water uptake and swelling, it also increases the tensile modulus of the films. This suggests that the films maintain an adequate moisture content while mitigating the dehydration risks associated with TiO2 nanotubes (NTs) alone.

Furthermore, the study found that wounds treated with the GG+TiO_2-NTs films healed faster compared to untreated wounds. The tensile strength and Young's modulus of the films were measured as (4.56 ± 0.15) MPa and (68 ± 1.63) MPa, respectively.

[31]. Additionally, some investigations have been conducted on polymers and biological systems. Over the past decades, polypyrrole as one of the popular types of conductive polymers (CPs) are used for tissue engineering and drug delivery application [32-35]. In research, polypyrrole nanoparticles (PPy–NPs) conjugated with conductive polymer of PCL (poly (ε-caprolactone) as an aliphatic polyester scaffold with good mechanical property for fabricating biocompatible scaffolds was investigated. PCL scaffolds show poor cell adhesion, migration, and proliferation, low hydrophilicity; and specifically, nothing conductive property. PCL/PPy conductive scaffold was applied in physical, mechanical, and biological fields. They used AFM for determining PCL/PPy composite roughness and mechanical parameters, and indicated that surface roughness of PCL/PPy composite was increased and Young's Modulus (2 to 4-folds) and tensile strength (3 to 4-folds) as mechanical strength parameters improved.

They showed that surface roughness improvement was depended to PPy–NPs concentration in the PCL/PPy composite scaffolds. Moreover, cell adhesion, growth, and proliferation were related to surface roughness [36].
Moreover, the metabolism and physiological activities of cells can be probed by deformability as an inherent property. Erythrocyte deformability indicates a strong relationship with erythrocyte aging. AFM using a V-shaped silicon nitride cantilever with a nominal spring constant of 0.06 N/m has been employed. By approaching the tip to the cell, passive and active deformation can be distinguished. Initially, the cell experiences zero force, and the transition from zero force to the separation of the tip-cell interaction is referred to as cell passive deformation and cell active deformation, respectively.
The erythrocytes exhibited the highest amounts of Young’s modulus for active deformation but the lowest amounts for passive deformation. Thus, the Young's modulus of erythrocytes is calculated as a primary mechanical specification for determining cell stiffness, serving as a novel biomechanical characteristic for monitoring aged erythrocytes. The average Young's modulus was measured at 1.27 kPa and 1.21 kPa at the center and terminal radius, respectively, over the erythrocyte surface [37].

Tang et al. identified the importance of passive and active deformations on the mechanical responses of erythrocytes, analyzing them through energy states.

The energy consumed during these deformations varied based on the age of the erythrocytes, with active deformation energy considered a crucial mechanical parameter for clearing and removing aged cells. Wounds, whether on the skin or other tissues, represent a significant health concern. Such injuries can damage the skin layer and compromise its protective system, potentially leading to infection, bleeding, sepsis, keloids, and scar formation. Therefore, the mechanical properties and antibacterial activity of wound dressings are essential for effective wound care.

Several metals such as silver, gold, copper, and titanium have been utilized to enhance the treatment of human cell diseases and wounds [38].

In a study, myricetin (MCE) and its glycoside myricitrin (MCI) flavonols (molecules that exhibit interesting biological activity) were selected, and the effects of interactions between 1,2-dimyristoyl-sn-glycero-3-phosphocholine (DMPC) bilayers and these flavonols were investigated through simulation studies. Flavonols, as an important part of human nutrition, are polyphenols with hydrophilic and/or hydrophobic properties, which can influence various cell membrane parameters such as fluidity by altering membrane enzyme activities and permeability [39].

The results indicate that the interaction between cell membranes and MCI flavonol is stronger than that with MCE flavonol. This difference can be attributed to the disparity in polarities between MCE and MCI [40].

Damaged tissues can be treated using biological methods, such as 3D artificial matrices or scaffolds. This process is referred to as tissue engineering (TE) [41]. These scaffolds should be made from materials with open porosity, which allows for controllable pore shape and size, and they must be biocompatible. The stiffness and permeability of the scaffold play significant roles in TE. In this context, AFM was employed to measure the mechanical properties of poly (ε-caprolactone) (PCL) fibers with varying diameters at both macro and nanoscale levels. Additionally, Young's modulus values were obtained using force-distance curves produced by AFM. The results indicated that variations in fiber diameters can significantly affect the mechanical properties of scaffolds, which is a critical factor in designing 3D-printed fibers [42].

Cancer is a serious issue among diseases and is regarded as a significant challenge in new researches. It is reported that a tumor can begin from possibly a single cell within a cluster of precancerous cells that contribute to oncogenic transformation [43].

Furthermore, the mechanical properties of cells, including tissue formation, cell functionality, and stem cell differentiation, are crucial factors in cancer diagnosis. In this regard, atomic force microscopy can be utilized to study cell mechanics, the pericellular coat, or the brush-like layer surrounding eukaryotic cells [44]. Atomic Force Microscopy (AFM) shows promise for enhancing our understanding of the factors responsible for cancer initiation. A study used AFM to explore the physical properties of cancer-initiating cells and surrounding tissues in three animal tumors. Identifying these factors could influence cancer onset and progression.

The study revealed a significant increase in the effective Young's modulus of surrounding tissues compared to cancer-initiating cells, indicating that surrounding tissues were stiffer. Notably, cancer-initiating cells exhibited softer properties than advanced cancer cells.

These AFM analyses of cell physical parameters demonstrated crucial changes associated with cancer development.

AFM indentation was employed to examine cancer-initiating cells and surrounding tissues as controls. Statistically significant differences were observed in the mechanical properties and effective Young's modulus between these groups. Importantly, cancer-initiating cells displayed a decrease in effective Young's modulus compared to surrounding tissues [45].

In research, scientists use atomic force microscopy (AFM) to study the properties of collagen fibrils. Tendon tensile strength and various other connective tissues stem from these collagen fibrils. Characterized by protein structures, collagen fibrils are rope-like supermolecules whose hierarchical structures are maintained by intermolecular and covalent bonds between individual molecules. To investigate single collagen fibrils from tendons, researchers have employed atomic force microscopy with high resolution and speed, along with a hydrated mechanical mapping technique.

They separated five fibrils from each tendon of five individual animals (a total of 25 fibrils) and mechanically investigated the fibrils from tendons in both hydrated and dehydrated states. Each fibril was imaged using AFM in both the dehydrated and rehydrated conditions. Fibril deformation at a point was described based on the force/distance curve. They demonstrated that all fibrils exhibited microscale variation, and the distribution of these variations along the length of the fibril was calculated. They proposed that the source of this variation in modulus is due to local differences in the number of collagen molecules per unit length and/or differences in crosslink density [46].

A study measured the nanoscale effects of various soft drinks on human tooth enamel using Atomic Force Microscopy (AFM). It focused on changes in roughness (Rq) and elastic modulus (E) over time by immersing teeth in different beverages.

By calculating the topography and elastic modulus, researchers aimed to identify early signs of enamel weakening, an essential step in understanding dental erosion. Dental erosion is caused by acidic foods and drinks, certain medications, and specific treatments. It removes hard dental tissue, leaving the enamel rough and weakened. This erosion allows bacteria and acids to penetrate the tooth structure, reaching the dentin and causing sensitivity to heat, cold, sweet, and sour foods. In some cases, it can even lead to hypersensitivity.The study's findings emphasize the importance of elastic modulus as a crucial factor in identifying the early stages of enamel weakening during the etching process [47].

AFM can strongly help identify mechanical and structural differences in each cell type [48,49]. Ngayama et al. studied the macroscopic and microscopic analysis of the mechanical properties, adhesion force, and cell-substrate adhesion strength of various cell types through AFM analysis. According to their results, the mechanical properties of vascular smooth muscle cells (VSMCs) were up to two times larger than those of HeLa cells. This is attributed to the internal tension and shape discipline of the actin cytoskeleton [50].

Three-dimensional biocompatible materials with sizes ranging from micro to nanoscale can be utilized for the bone formation process or neural tissue reconstruction, as they are sensitive to the mechanical properties of the substrates. In their research, Buchroithner et al. studied the mechanical properties of biocompatible materials using AFM. They measured the Young's modulus of two biocompatible resins (pentaerythritol triacrylate (PETA) and hybrid OrmoComp monomers) and compared it to that of two resins commonly used in multiphoton lithography. The Young's modulus value is reported to be in the range of 100 MPa. They indicated that the Young's modulus of OrmoComp was the smallest, which is attributed to its high aspect ratio [51].
Worldwide, one of the deadliest diseases is glioblastoma (GBM). Hohman et al. studied the effect of Metastasis-associated in colon cancer 1 (MACC1), which can increase the migration speed of single cells and their elastic modulus, leading to decreased adhesion and increased elasticity. First, cells were allowed to adhere to a petri dish, and after starting the test, single cells were examined using an AFM tip to identify their Young’s modulus.

Additionally, the average diameter of the cell was measured, providing a good estimate of the initial cell-cell distance. The observed changes in adhesion, elasticity, and tension lead to inhibited GBM cell migration and thus an improvement in the disease [52].

6. Application of AFM in the Young's modulus determination in the unbiological science

Some investigations were done on nano materials. Short fiber reinforced rubber composites have significant properties, which they can applied for diverse industrial applications. The interfacial interaction and interfacial nanomechanical properties between fibers and rubber can affect on interface quality as a key factor for the increasing of efficiency, the mechanical properties and failure behavior of the composites. Tian et al. studied interfacial interaction of three kinds fibrillar silicate/elastomer nanocomposites (FS/NR) by combination of quantitative nanomechanical technique and atomic force microscopy (AFM-QNM). These nanocomposites exhibited excellent performance, which their mechanical properties and Young's modulus were quantitatively determined via AFM-QNM. Interfacial thickness and Young's modulus of the modified FS/NR composites were higher than unmodified-FS/NR composites. This could be ascribed to presence of chemical bonds and physical entanglement between modified-FS and NR matrix and between unmodified-FS and NR matrix, respectively. This research can provide to deep comprehend the interface of nanofiber reinforced composites, and it can help to design of interfacial high performance rubber composites [53].

Hyperbranched polyglycerols (hbPGs) are highly biocompatible materials due to their high molecular weight. Various analytical techniques were used to characterize the synthesized materials, which have also been explored for drug delivery applications [54-55]. Atomic Force Microscopy (AFM) offers a powerful tool to measure the Young's modulus, adhesion force in molecular bonds, and surface chemical state of hbPGs, making them an attractive polymer for drug delivery. A study reported that the Young's modulus of hbPGs strongly increased when deposited on a mica substrate, which was attributed to the formation of intramolecular hydrogen bonds [56].

Textile wastewater often contains dyes and other chemicals that must be removed before discharge to protect the environment. Membrane technology, including ultrafiltration (UF) and nanofiltration (NF), offers a promising approach for this purpose due to its economic viability, high removal efficiency, and minimal environmental impact. However, these membranes can experience fouling, which reduces their effectiveness.

Modifying the membranes with nanoparticles provides a new method to enhance their surface properties and reduce fouling. Sakarkar et al. investigated the use of six different polyvinyl alcohol (PVA)/titanium dioxide (TiO2) composite membranes coated on polyvinylidene fluoride (PVDF) for dye removal from textile wastewater using the dip-coating method. They compared the mechanical properties of these composite membranes. Their results showed that the root mean square roughness of the pure PVDF membrane was 1.067 nm, while the composite membrane containing 12 wt% PVA exhibited a significantly higher roughness of 120 nm [57].

Moreover, using the SEM, AFM, FTIR, XRD and contact angle results, the interactions between TiO_2 nanoparticles and PVA in the coating were detected, which led to changed surface morphologies and increased hydrophilicity of the membranes [57].

Some research has been done on polymers and non-biological science. Fang et al. studied the Young's modulus of the membranes of natural oil bodies (OBs) such as soybean, sesame, and peanut using AFM. They demonstrated that membrane structure and surface molecular conformation can lead to differences in the mechanical properties of the various OBs. A higher protein/oil ratio in OBs can result in smaller size, stronger mechanical traits, and greater stability, making these properties beneficial for membrane applications in industry [58].

Diamond-like carbon (DLC) films, valued for their semiconducting properties, were successfully deposited on Si substrates using helicon wave plasma chemical vapor deposition (HW-PCVD) with Ar/CH4 mixtures at room temperature. These films demonstrate high biocompatibility, hardness, chemical resistance, electrical resistivity, and low friction coefficients, making them suitable for various electronic applications.

The influence of CH4 flow rate (ranging from 5 to 25 sccm) on the surface energy of the DLC films was investigated using Atomic Force Microscopy (AFM). The films achieved the highest Young's modulus of 11 GPa at a CH4 flow rate of 25 sccm, attributed to the presence of C-C sp3 bonds. Interestingly, the AFM study also revealed that the DLC film surfaces were relatively soft [59].

In fact, increasing the PVA value led to enhanced tensile strength and Young's modulus of the coated membranes, due to the agglomeration of TiO2 nanoparticles in the composite, which can increase roughness. Additionally, dye removal is more common for high molecular weight dye molecules because they become trapped in small membrane pores.

The valorization of natural resources can help address environmental problems caused by the excessive use of fossil resources. Lignin-containing cellulose nanofibers (LCNFs), as lignocellulosic materials, are viewed as a suitable option for applications in composites, biomedical devices, filtration, and packaging.

Yang et al. produced LCNFs from wheat residues, which were then integrated into a polyvinyl alcohol (PVA) matrix. The incorporation of LCNFs in the PVA composite films led to significant enhancements in tensile strength, Young's modulus, thermal resistance, surface properties, and a slight reduction in elongation at break. Therefore, LCNFs are anticipated to be excellent candidates for a variety of applications, including use as additives in composites and biomedical devices, among others [60].

Glass molding is an effective and environmentally friendly method for producing optical elements such as aspheric lenses. Optical elements are manufactured with various coatings, including metal or nitride, on a range of surfaces for glass molding applications [61-62]. A previous study by Li et al. investigated the effect of CrxWyNz coatings on cemented carbide (WC-8Co) under thermal-mechanical cycles in a nitrogen atmosphere. CrxWyNz coatings were deposited on WC-8Co using plasma-enhanced magnetron sputtering (PEMS) technology and subsequently evaluated for their performance in a precision glass molding machine (PGMM). Atomic Force Microscopy (AFM) was used to assess the mechanical properties of the coated surfaces.

The study found that increasing the W content in the CrxWyNz coatings led to a simultaneous increase in Young's modulus and a decrease in surface roughness. Additionally, the coatings protected against oxidation reactions during the thermal-mechanical cycles, resulting in reduced surface roughness in the contact area compared to the non-contact area. Overall, the study concluded that CrxWyNz coatings (with $18 \leq x \leq 27$ and $24 \leq y \leq 28$) represent a suitable protective coating for this application [63].

The mechanical properties of titanium carbon nitride (TiCN) coatings have been investigated by several researchers in recent years because TiCN exhibits greater hardness than commercial TiAlN and TiN coatings [64].

Das et al. synthesized TiCN thin films on Si substrates using the CVD technique under varying N2 gas flow rates (6-15 sccm) and evaluated the effectiveness of the CVD method for growing TiCN coatings on machine components at high temperatures.

Various analyses were conducted to identify the morphological, structural, corrosion behavior, and mechanical properties of the coatings. AFM analysis was employed to determine the surface roughness. The results indicated that increasing the N2 flow rate enhanced the hardness (H), Young's modulus (E), and particle size. The nanoindentation results showed an increase in coating hardness and Young's modulus with rising N2 flow rates, ranging from 23.85±1.87 to 27.88±1.86 sccm and from 449.65 to 486.22 GPa, respectively. An increased N2 flow rate resulted in reduced coating roughness. The maximum surface roughness and Young's modulus were reported at 48.25 nm and 486.22 GPa at low and high flow rates, respectively [65].

7. Conclusion

Atomic force microscopy (AFM) has emerged as a powerful technique in both scientific and industrial fields, enabling the study of various physical and structural properties of compounds at the nanoscale. One key strength of AFM is nano-indentation, which allows for accurate measurement of Young's modulus, providing valuable quantitative information about the mechanical properties and nature of materials. This rapidly growing field of knowledge holds immense potential for a deeper understanding of mechanical characteristics at the molecular and atomic scales. Beyond its impressive mechanical characterization capabilities, AFM's ease of use and non-destructive nature have cemented its position as a critical tool in biology and surface science research. Furthermore, its versatility across diverse applications, along with its exceptional nanoscale resolution, makes AFM an increasingly popular choice in both research and industrial settings.

References

[1] Panitz, J. S. P., Desenvolvimento e implementação de metodologias para a determinação da deformabilidade e tensões em maciços gn´aissicos, Pontif´ıcia Universidade Cat´olica Do Rio De Janeiro. Rio de Janeiro, Brazil. IJM, P. 2007; 11: 1096-1109.

[2] Bezerra, M. T. P. A., Silva, F. M., de Souza Soares, M. M. N., Relações do mo´dulo de elasticidade dinaˆmico, esta´tico e resisteˆncia a` compressão do concreto. Anais do 51° Congresso Brasileiro do Concreto–IBRACON. J. Augusto Cesar da Silva. 2009; 20: 1-10.

[3] Chang, Y. R., Raghunathan, V. K., Garland, S. P., Morgan, J. T., Russel, P., Murphy, C. J., Automated AFM force curve analysis for determining elastic modulus of biomaterials and biological samples. J. Mech. Behav. Biomed. Mater. 2014; 37: 209–218.

[4] Putman, C. A. J., Van der Werf K. O., De Grooth B. G., Van Hulst N. F., Greve J., Tapping mode atomic force microscopy in liquid. J. Appl. Phys. Lett. 1994; 64: 2454.

[5] Weymouth, A. J., Wastl, D., Giessibl, F. J., Advances in AFM: seeing atoms in ambient conditions. e-J. Surf. Sci. Nanotech. 2018; 16: 351–355.

[6] M. Hua, Y., Y. Han, C., Y. Shiuan, L., O. Sheng, L., Alteration of Young's modulus in mesenchymal stromal cells during osteogenesis measured by atomic force microscopy. B. B. R. C. 2020; 526: 827-832.

[7] Fuzhou, T., Dong, C., Shichao, Z., Wenhui, H., Jin, C., Houming, Z., Zhu, Z., Xiang, W., Elastic hysteresis loop acts as cell deformability in erythrocyte aging. J. BBA – Biomembranes. 2020; 1862: 183309.

[8] Majewskaa, M., Mrdenovica, D., Pietaa, I.S., Nowakowskia, R., Pietaa, P., Nanomechanical characterization of single phospholipid bilayer in ripple phase with PF-QNM AFM. BBA – Biomembranes. 2020; 1826: 183-347.

[9] Hermanowicz, P., Determination of Young's modulus of samples of arbitrary thickness from force distance curves: numerical investigations and simple approximate formulae, International Journal of Mechanical Sciences, 2020.

[10] Zee Ma, Y., Janz, R., Glossary for Unconventional Oil and Gas Resource Evaluation and Development. In Unconventional Oil and Gas Resources Handbook. 2016.

[11] Sirohi, R. S. A., Course of Experiments with He-Ne laser. Wiley Eastern Limited, New Delhi. 1986; 67.

[12] Sadegh Hassani, S., Afzali, J., Khosravi, M., Atomic force microscopy. Gisoom publisher Aug. 2014.

[13] Sobat, Z., Sadegh Hassani, S., An overview of scanning near field optical microscopy in characterization of nanomaterials. Int. J. Nano. Dim. 2014; 5: 203-308.

[14] Sadegh Hassani, S., Scanning tunneling microscopy and its application under electrochemical conditions. J. RIPI Publisher. 2011; 2.

[15] Sadegh Hassani, S., Daraee, M., Sobat, Z., Application of atomic force microscopy in adhesion force measurements. J. Adhes Sci Technol. 2021; 35: 221-241.

[16] Kaman, J., Young's Modulus and Energy Dissipation Determination Methods by AFM, with Particular Reference to a Chalcogenide Thin Film, Periodica Polytechnica Electrical Engineering and Computer Science, 2015, 59(1).

[17] Sadegh Hassani, S., Sobat, Z., Aghabozorg, H. R., Scanning probe lithography as a tool for studying various surfaces. NSNTAIJ. 2008; 2: 94-98.

[18] Sadegh Hassani, S., Aghabozorg, H. R., Recent Advances in Nanofabrication Techniques and Applications. Chapter title: Nanolithography Study Using Scanning Probe Microscope. InTech publisher. 2011.

[19] Tick Boon Loh, Yutong Wu, Siang Huat Goh, Kian Hau Kong, Kheng Lim Goh and Jun Jie Chong, Jun Jie Chong, An Integrated Approach for the Determination of Young's Modulus of a Cantilever Beam Using Finite Element Analysis and the Digital Image Correlation (DIC) Technique, *Electronics* 2022, *11*(18), 2826.

[20] Roa, J. J., Oncins, G., Diaz, J., Sanz, F., Segarra, M., Calculation of Young's Modulus Value by Means of AFM. J. Recent Pat Nanotechnol. 2011; 5: 27-36.

[21] J. Price, W., A. Leigh, S., M. Hsu, S., E. Patten, T., Liu, G. Y., Measuring the Size Dependence of Young's Modulus Using Force Modulation Atomic Force Microscopy. J. Phys. Chem. A. 2006; 110: 1382-1388.

[22] I. Krymskaya, K., V. Andreeva, N., V.Filimonov, A., A technique for determining Young's modulus of biological objects using atomic-force microscopy in the wide temperature range below Rt. 2016; 2: 217-223.

[23] Maugis, D., Barquins, M., Adhesive contact of sectionally smooth-ended punches on elastic half space theory and experiment. J. Phys. D. Appl. Phys. 1983; 16: 1843.

[24] Li, M., Xi, N., Wang, Y., Advances in atomic force microscopy for single-cell analysis, J. Nano Res. 2019; 12: 703-718.

[25] N. Patel, A., Kranz, C., (Multi) functional Atomic Force Microscopy Imaging. in Annual Review of Analytical Chemistry. Annual Review of Analytical Chemistry. J. Palo Alto: Annual Reviews. 2018; 11:329-350.

8. [26] Yunkyung, L., Manhee, L., Sangmin, A., Sang-Joon, C., Quantitative Visualization of the Nanomechanical Young's Modulus of Soft Materials by Atomic Force Microscopy Seongoh Kim. Nanomaterials. 2021; 11: 1593.

[27] Yuta, N., Yukihiro, Y., Yuki, H., Yoshitaka, N., Method for measuring Young's modulus of cells using a cell compression microdevice Tairo Yokokura. Int J Eng Sci. 2017; 114: 41-48.

[28] K. Dimitriadis, E., Horkay, F., Maresca, J., Kachar, B., S. Chadwick, R., Determination of Elastic Moduli of Thin Layers of Soft Material Using the Atomic Force Microscope. Biophys. J. 2002; 82: 2798–2810.

[29] M. Hua, Y., Y. Han, C., Y. Shiuan, L., O. Sheng, L,. Alteration of Young's modulus in mesenchymal stromal cells during osteogenesis measured by atomic force microscopy. B. B. R. C. 2020; 526: 827-832.

[30] Mazzini, A., Palermo, F., Pagliei, V., Romano, S., Papi, M., Zimatore, G., Falsini, B., Rizzo, S., D. Spirito, M., Ciasca, G., M. Minnella, A., A time-dependent study of nano-mechanical and ultrastructural properties of internal limiting membrane under ocriplasmin treatment. J. Mech Behav Biomed Mater. 2020; 110: 103853.

[31] M. Hasmizam, R., N. Afrifah, I., K. A. Mat, A., Titanium dioxide nanotubes incorporated gellan gum bio-nanocomposite film for wound healing: Effect of TiO2 nanotubes concentration. Int. J. Biol. Macromol. 2020; 153: 1117-1135.

[32] Xiangru, F., Jiannan, L., Xi, Z., Tongjun, L., Jianxun, D., Xuesi, C., Electrospun polymer micro/nanofibers as pharmaceutical repositories for healthcare, J. Control. Release. 2019; 302: 19–41.

[33] T. I, H., J. I, K., M. Kumar, J., C. Hee, P., C. Sang, K., Simultaneous regeneration of calcium lactate and cellulose into PCL nanofiber for biomedical application, J. Carbohydr. Polym. 2019; 212: 21–29.

[34] P. Bhattarai, P., P. Tiwari, A., Maharjan, B., Tumurbaatar, B., H. Park, C., S. Kim, C., Sacrificial template-based synthetic approach of polypyrrole hollow fibers for photothermal therapy. J. Colloid Interface Sci. 2019; 534: 447–458.

[35] T. Hai, L., Yukyung, K., Hyeonseok, Y., Electrical and Electrochemical Properties of Conducting Polymers. J. Polym. 2017; 9: 9040150.

[36] Maharjan, B., K. Kaliannagounder, V., S. Rim, J., G. Prasad. A., D. Prasad, B., Ghizlane, C., H. Park, C., C. Sang. K., In-situ polymerized polypyrrole nanoparticles immobilized poly(ε-

caprolactone) electrospun conductive scaffolds for bone tissue engineering. J. Mater. Sci. Eng. C. 2020; 114: 111056.

[37] Fuzhou, T., Dong, C., Shichao, Z., Wenhui, H., Jin, C., Houming, Z., Zhu, Z., Xiang, W., Elastic hysteresis loop acts as cell deformability in erythrocyte aging. J. BBA – Biomembranes. 2020; 1862: 183309.

[38] V. Giang, N., Hoang, T., D. Huynh, M., H. Trung, T., D. Lam, T., M. T, Vu., Effect of titanium dioxide on the properties of polyethylene/TiO_2 nanocomposites. J. Compos. B. 2013; 45: 1192–1198.

[39] Selvaraj, S., Krishnaswamy, S., Devashya, V., Sethuraman, S., M. Krishnan, U., Influence of membrane lipid composition on flavonoid–membrane interactions: implications on their biological activity, J. Prog. Lipid Res. 2015; 58: 1–13.

[40] Sadžak, A., Brkljača, Z., Crnolatac, I., Baranović, G., Šegota, S., Flavonol clustering in model lipid membranes: DSC, AFM, force spectroscopy and MD simulations study, J. Colloids and Surfaces B: Biointerfaces. 2020; 193: 111147.

[41] Idaszek, J., Kijeńska, E., Łojkowski, M., Swieszkowski, W., How important are scaffolds and their surface properties in regenerative medicine, J. Appl. Surf. Sci. 2016; 388: 762–774.

[42] Gorecka, Z., Idaszek, J., Kołbuk, D., Choińska, E., Chlanda, A., Święszkowski, W., The effect of diameter of fibre on formation of hydrogen bonds and mechanical properties of 3D-printed PCL. Mater. Sci. Eng. C. 2020; 114: 111072.

[43] Sokolov, I., Dokukin, M. E., Kalaparthi, V., Miljkovic, M., Wang, A., Seigne, J. D., Grivas, P., Demidenko, E., Noninvasive diagnostic imaging using machine-learning analysis of nanoresolution images of cell surfaces: detection of bladder cancer. J. Proc. Natl. Acad. Sci. U.S.A. 2018; 115: 12920–12925.

[44] Wu, P. H., R. B. Aroush, D., Asnacios, A., Chen, W. C., E. Dokukin, M., L. Doss, B., D. Smet, P., Ekpenyong, A., Guck, J., V. Guz, N., A. Janmey, P., S. H. Lee, J., M. Moore, N., Ott, A., Poh, Y. C., Ros, R., Sander, M., Sokolov, I., R. Staunton, J., Wang, N., Whyte, G., Wirtz, D., A comparison of methods to assess cell mechanical properties. J. Nat. Methods 15. 2018; 491–498.

[45] Makarova, N., Vivek, K., Andrew, W., Chris, W., Dokukin, M. E., K. Kaufman, C., Zon, L., Sokolov, I., Difference in biophysical properties of cancer-initiating cells in melanoma mutated zebrafish. J. Mech Behav Biomed Mater. 2020; 107: 103746.

[46] J. Baldwin, S., Sampson, J., J. Peacock, C., L. Martin, M., P. Veres, S., Lee, J. M., Kreplak, L., A new longitudinal variation in the structure of collagen fibrils and its relationship to

locations of mechanical damage susceptibility. J. Mech Behav Biomed Mater. 2020; 110: 103849.

[47] Panpan, Li., Chungik, O., Hongjun, K., Melodie, C. G., Gun, P., Albina, J., Jiwon, Y., Hoon, K., Jeongjae, R., Seungbum, H., Nanoscale effects of beverages on enamel surface of human teeth: An atomic force microscopy study. J. Mech Behav Biomed Mater. 2020; 110: 103930.

[48] Urbanska, M., Winzi, M., Neumann, K., Abuhattum, S., Rosendahl, P., Müller, P., Taubenberger, A., Anastassiadis, K., Guck, J., Single-cell mechanical phenotype is an intrinsic marker of reprogramming and differentiation along the mouse neural lineage. J. Development. 2017; 144: 4313–4321.

[49] Vahabikashi, A., Park, C. Y., Perkumas, K., Zhang, Z., K. Deurloo, E., Wu, H., A. Weitz, D., Stamer, W. D., D. Goldman, R., J. Fredberg, J., Johnson, M., Probe sensitivity to cortical versus intracellular cytoskeletal network stiffness. J. Biophys. 2019; 116: 518–529.

[50] Kazuaki, N., Shigeaki, O., Shota, O., Akiko, S., Macroscopic and microscopic analysis of the mechanical properties and adhesion force of cells using a single cell tensile test and atomic force microscopy: Remarkable differences in cell types. J. Mech Behav Biomed Mater. 2020; 110: 103935.

[51] Buchroithner, B., Hartmann, D., Mayr, S., Oh, Y. J., Sivun, D., Karner, A., Buchegger, B., Griesser, T., Hinterdorfer, P., A. Klarb, T., Jacak, J., 3D multiphoton lithography using biocompatible polymers with specific mechanical properties, J. Nanoscale Adv. 2020; 2: 2422.

[52] Offroy, M., Razafitianamaharavo, A., Beaussart, A., Pagnoutb, C., F. L. Duval, J., Fast automated processing of AFM Peak Force curves to evaluate spatially resolved Young modulus and stiffness of turgescent cells, J. RSC Adv. 2020; 10: 19258.

[53] Chenchen, T., Yuxing, F., Guangyu, C., Yonglai, L., Chunmeng, M., Nanying, N., Liqun, Z., Ming, T., Interfacial nanomechanical properties and chain segment dynamics of fibrillar silicate/elastomer nanocomposites. J. Composites Part B 193. 2020; 108048.

[54] Schön, P., Görlich, M., J. J. Coenen, M., A. Heus, H., Speller, S., Nonspecific protein adsorption at the single molecule level studied by atomic force microscopy, J. Langmuir. 2007; 23: 9921–9923.

[55] Meng, L., Jinjie, Z., Nianwa, T., Hang, S., Jinling, H., Horizontal gene transfer from bacteria and plants to the arbuscular mycorrhizal fungus Rhizophagus irregularis, J. Front. Plant Sci. 2018; 9: 701.

[56] Haigang, W., Qunzhi, C., Mingzhu, J., Xue, X., Xueyan, L., Nan, H., Ke, L., Jinlong, Y., Bingyang, S., Evaluation of nanomechanical properties of hyperbranched polyglycerols as

prospective cell membrane engineering block, J. Colloids and Surfaces B: Biointerfaces. 2020; 190: 110968.

[57] Sakarkar, S., Muthukumaran, S., Jegatheesan, V., Evaluation of polyvinyl alcohol (PVA) loading in the PVA/titanium dioxide (TiO2) thin film coating on polyvinylidene fluoride (PVDF) membrane for the removal of textile dyes, J. Chemosphere. 2020; 257: 127144.

[58] Yang, N., Su, C., Zhang, Y., Jia, J., L. Leheny, R., Nishinari, K., Fang, Y., O. Philips, G., In situ nanomechanical properties of natural oil bodies studied using atomic force microscopy. J. Colloid Interface Sci. 2020; 570: 362–374.

[59] Jia-li, C., Pei-yu, J., Yan, Y., C. Gang, J., L. Jian, Z., X. Mei, W., The structure and properties of amorphous diamond-like carbon films deposited by helicon wave plasma chemical vapor deposition. J. Thin Solid Films. 2020; 709: 138167.

[60] Mingyan, Y., Xiao, Z., Shuyi, G., Yan, D., Xiaofeng, G., Preparation of lignin containing cellulose nanofibers and its application in PVA nanocomposite films. Int. J. Biol. Macromol. 2020; 158: 1259–1267.

[61] S. Hong, L., I. Hwan, K., T. Youn, K., Surface failure analysis of AlCrN coating on WC substrate subjected to high-temperature oxidation in glass-molding machine, J. Appl. Surf. Sci. 2018; 405: 210–216.

[62] X. Yan, Z., J. Jun, W., L. Xian, C., J. Long, L., L. Fu, H., C. Ming, L., Yong, Z., Anti-sticking Re-Ir coating for glass molding process, J. Thin Solid Films. 2015; 584: 305–309.

[63] Kangsen, L., Gang, X., Xinfang, H., Qiang, C., Zhiwen, X., Feng, G., Surface evolution analysis of CrxWyNz coatings on WC mold in glass molding Process. J. Surf. Coat. Technol. 2020; 393: 125839.

[64] Bull, S. J., Bhat, D. G., Staia, M. H., Properties and performance of commercial TiCN coatings Part 1: coating architecture and hardness modelling, J. Surf. Coat. Technol. 2003; 163–164: 499–506.

[65] Soham, D., Spandan, G., P. Protim, D., Ranjan, K. G., Analysis of morphological, microstructural, electrochemical and nano mechanical characteristics of TiCN coatings prepared under N_2 gas flow rate by chemical vapour deposition (CVD) process at higher temperature. J. Ceram. Int. 2020; 46: 10292–10298.